Available online at www.sciencedirect.com
ScienceDirect
Journal of Photochemistry and Photobiology A: Chemistry 183 (2006) 205–211
Journal of Photochemistry and Photobiology A:Chemistry
www.elsevier.com/locate/jphotochem

Nitrile-forming radical elimination reactions of 1-naphthaldehyde *O*-(4-substituted benzoyl)oximes activated by triplet benzophenone

Koji Yamada [a], Masaru Sato [a], Kenta Tanaka [b], Azusa Wakabayashi [a], Tetsutaro Igarashi [a], Tadamitsu Sakurai [a,*]

[a] *Department of Applied Chemistry, Faculty of Engineering, Kanagawa University, Kanagawa-ku, Yokohama 221-8686, Japan*
[b] *High-Tech Research Center, Kanagawa University, Kanagawa-ku, Yokohama 221-8686, Japan*

Received 6 January 2006; received in revised form 22 February 2006; accepted 18 March 2006
Available online 30 March 2006

Abstract

It was found that 1-naphthaldehyde *O*-aroyloximes (**1**) preferentially adopting the *anti*-configuration undergo efficient triplet-sensitized reactions to give 1-cyanonaphthalene and monosubstituted benzenes as unimolecular radical elmination products along with *syn*-**1**. Negligible formation of 4-substituted benzoic acids strongly suggested the participation of simultaneous N–O and C(=O)–Ar bond cleavages in the triplet excited-state *anti*-isomer. The logarithm of the $k_r/(k_d + k_i)$ ratio (where k_r is the rate constant for homolytic bond cleavage in triplet **1**, k_d the rate constant for deactivation of the triplet *anti*-isomer, and k_i is the rate constant for isomerization of triplet *anti*-**1** into *syn*-**1**) used as a measure of the triplet-state reactivity of *anti*-**1** showed a negligible dependence on the substituent constant and solvent polarity. This finding was explained in terms of a very small contribution of the ionic structure to the transition-state for simultaneous N–O and C(=O)–Ar bond cleavages.

Keywords: 1-Naphthaldehyde *O*-acyloximes; Triplet-sensitized photolysis; Radical elimination; Substituent and solvent effects; Transition-state structure

1. Introduction

Thus far much effort has been devoted to mechanistic studies regarding imine- [1–6] and nitrile-forming [7–10] elimination reactions and has enabled the observation of important mechanistic differences between these reactions and alkene- and alkyne-forming eliminations [11–13]. In contrast with bimolecular and ionic imine- and nitrile-forming eliminations, there has been no study regarding these radical elimination reactions. During the course of our systematic study of the direct and sensitized photolyses of *N*,*O*-diacyl-*N*-phenylhydroxylamines [14,15], we found that the hydroxylamines readily undergo an N–O bond homolysis in the triplet excited-state, giving aminyl and aroyloxyl radicals. If there exists hydrogen at the α-position of the aminyl nitrogen atom, the aroyloxyl radical could abstract this hydrogen, yielding imine and carboxylic acid as unimolecular radical elimination products. From this point of view, we previously designed *N*,*N*-dibenzyl-*O*-(4-substituted benzoyl)hydroxylamines and investigated the triplet-sensitized photolysis of these hydroxylamines, hoping to find a new type of imine-forming radical elimination [16,17]. Analyses of substituent and deuterium isotope effects on the quantum yield for the reaction revealed that a caged singlet radical pair, in which hydrogen abstraction occurs affording elimination products, is involved in the reaction as a key intermediate. In addition, taking into account the fact that the 1-naphthoyl group becomes a far more effective triplet energy acceptor than the substituted benzoyl [14,15], we designed *N*,*N*-bis(4-substituted benzyl)-*O*-(1-naphthoyl)hydroxylamines and investigated substituent effects on the benzophenone(BP)-sensitized photolysis of these hydroxylamines in acetonitrile [18]. It was shown that despite the occurrence of a diffusion-limited triplet energy transfer, the triplet-state hydroxylamines decompose inefficiently giving 4-substituted *N*-(4-substituted benzylidene)benzylamines and 1-naphthoic acid as unimolecular radical elimination products. The finding that the substituents exert negligible electronic effects on the triplet-state reactivity led us to propose a very small contribution of the ionic structure to the transition-state for the N–O bond homolysis in the triplet excited-state. Thus, our previous results predict that the transition-state structure for

* Corresponding author. Fax: +81 45 491 7915.
E-mail address: sakurt01@kanagawa-u.ac.jp (T. Sakurai).

1010-6030/$ – see front matter © 2006 Elsevier B.V. All rights reserved.
doi:10.1016/j.jphotochem.2006.03.019

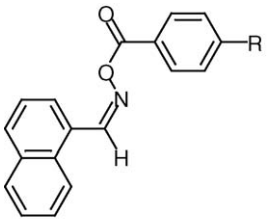

R = OMe (**1a**), Me (**1b**), H (**1c**), F (**1d**), Cl (**1e**)

Chart 1.

homolytic cleavage of the N–O bond is strongly dependent on the electronic state of a given hydroxylamine derivative in its triplet excited state. In order to secure a comprehensive understanding of the transition-state structure for radical eliminations, it is of great significance to extend our mechanistic study of the imine-forming radical elimination. Taking into account the possibility that 1-naphthaldehyde *O*-aroyloxime derivatives may undergo efficient triplet-sensitized photolysis to give N–O bond cleavage-derived radical elimination products, we designed and synthesized 1-naphthaldehyde *O*-(4-substituted benzoyl)oximes (**1a–e**) for the exploration of nitrile-forming radical elimination, hoping to shed much light on the transition state of the N–O bond cleavage (Chart 1).

2. Results and discussion

2.1. Conformational and product analyses

A ^{1}H NMR spectral analysis of the starting 1-naphthaldehyde oxime derivatives (**1**) showed that the *O*-acylation of 1-naphthaldehyde oxime with aromatic acyl chlorides gives **1** having a single configuration, namely, *syn*-**1** or *anti*-**1**. In order to determine the configuration of this isomer, we searched for energy-minimized configurations for *syn*-**1** and *anti*-**1** and estimated their heats of formation (ΔH_f). As typically shown in Fig. 1, *anti*-**1b** is thermodynamically more stable than *syn*-**1b** by 7.2 kJ mol^{-1}, confirming that **1** adopts the *anti*-configuration. In addition, careful inspection of both the energy-minimized configurations reveals that there is a large difference in the spatial distance between the iminomethyl proton (N=CH) and the naphthalene ring proton at the 2- (H^2) or 8-position (H^8) for the *syn*- and *anti*-isomers. The spatial distances between the N=CH proton and the H^2 and between the N=CH proton and the H^8 in *anti*-**1b** are 3.02 and 3.04 Å, respectively while these distances in *syn*-**1b** are 3.55 and 2.32 Å, respectively. This finding allows us to predict that if **1b** adopts the *anti*-configuration, the CH=N proton exhibits the difference NOE toward the H^2 and H^8 to nearly the same extent whereas such a NOE is not observed for *syn*-**1b**. The result of NOE analysis given in Fig. 2 is consistent with our prediction and, hence, provides additional evidence in support of the above assignment: *anti*-configuration. It is unlikely that the other substituents introduced into the benzoyl benzene ring greatly affect the relative stability of *anti*-**1b** and *syn*-**1b**, so that in any oxime derivatives the *anti*-isomers are considered to be thermodynamically more stable than the corresponding *syn*-isomers.

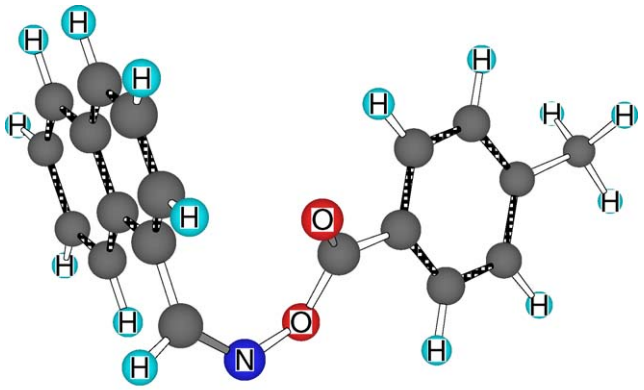

Anti-**1b** (ΔH_f = 74.3 kJ mol^{-1})

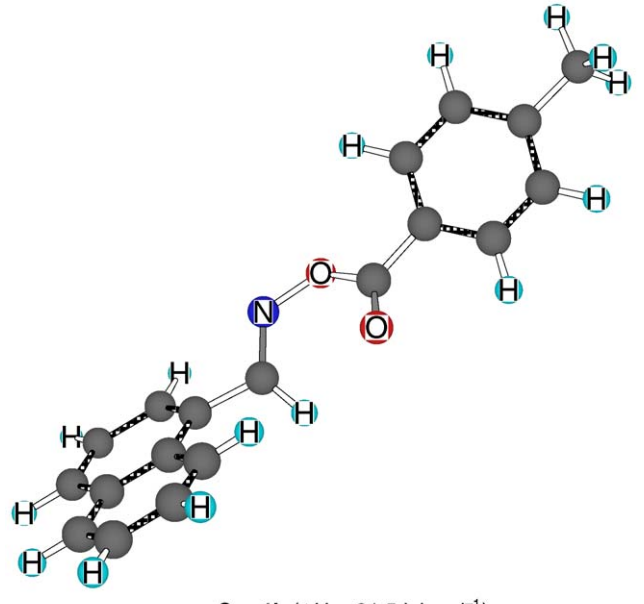

Syn-**1b** (ΔH_f = 81.5 kJ mol^{-1})

Fig. 1. Energy-minimized configurations of *anti*-**1b** and *syn*-**1b** and their heats of formation.

For the purpose of examining product distribution derived from the BP-sensitized photolysis of *anti*-**1**, a nitrogen-saturated acetonitrile solution of *anti*-**1b** (1.0×10^{-3} mol dm^{-3}) containing BP (3.0×10^{-2} mol dm^{-3}) was irradiated at 366 nm for a given period of time at room temperature and was subjected to HPLC analysis. On irradiation there appeared two new HPLC signals on the chromatogram, in addition to those of *anti*-**1b** and BP, whereas the signal for 4-toluic acid was not detected at any conversions of the starting *anti*-**1b**. One of the products was identified as 1-cyanonaphthalene (**2**) by comparing its HPLC behavior with that of authentic sample under several analytical

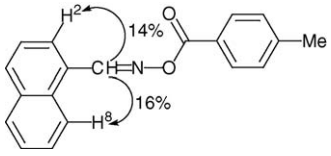

Fig. 2. Difference NOE analysis of the starting 1-naphthaldehyde oxime **1b**.

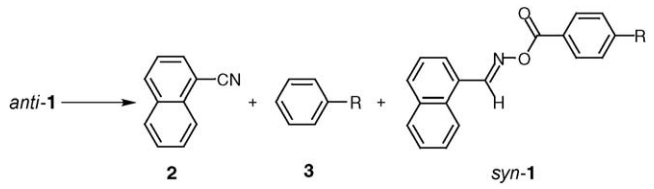

Scheme 1. Product distribution obtained by the BP-sensitized photolysis of *anti*-**1** in acetonitrile.

conditions. Since the unexpected product had been observed, we attempted to isolate this product. Fortunately the direct irradiation of *anti*-**1b** (1.0×10^{-3} mol dm^{-3}) in acetonitrile selectively afforded the unidentified photoproduct up to at least 40% conversion (HPLC analysis). In addition, the decrement of HPLC signal area of *anti*-**1b** is nearly equal to the increment of that of this photoproduct (data not shown) which slowly reverts to the starting **1b** on allowing the irradiated solution to stand at room temperature, suggesting the progress of photoisomerization to thermodynamically less stable *syn*-**1b**. Strong support for this suggestion comes from the finding that the unexpected product has the same number of protons and carbons and then gives the same area ratio of ^{1}H NMR signals as the *anti*-isomer does. Attempts to measure the difference NOE of *syn*-**1b** were unsuccessful owing to its slow conversion into the *anti*-isomer. On the other hand, no formation of 4-toluic acid indicates the exclusive progress of decarboxylation of the toluoyloxyl radical obtained by the homolytic N–O bond cleavage in the excited-state *anti*-**1b**. GLC analysis of the irradiated acetonitrile solution enabled the detection of this decarboxylation-derived product, toluene (**3b**), the GC behavior of which was compatible with that of authentic sample. The other starting *anti*-isomers gave the same product distribution as that arising from *anti*-**1b** (Scheme 1). In addition, the observation that HPLC behavior of *anti*-**1a**, **c**–**e** and *syn*-**1a**, **c**–**e** is almost the same as that of *anti*-**1b** and *syn*-**1b**, respectively, also substantiates the above-mentioned configurational assignment for these two isomers.

2.2. Phosphorescence quenching of BP and concentration dependence of quantum yields

As shown in Fig. 3, the room-temperature phosphorescence of BP (the first triplet excitation energy, $E_T = 290$ kJ mol^{-1}; the first singlet excitation energy, $E_S = 311$ kJ mol^{-1} [19]) was quenched by *anti*-**1b** according to the Stern–Volmer equation: $I_0/I = 1 + k_t\tau_T$[*anti*-**1b**] in which I, I_0, k_t, and τ_T are the emission intensity of BP with *anti*-**1b**, the emission intensity of BP without *anti*-**1b**, the rate constant for triplet-triplet energy transfer, and the lifetime (26 μs [20]) of triplet BP without *anti*-**1b**, respectively. The E_T value of *anti*-**1b** (224 kJ mol^{-1}) was estimated from the 0–0 peaks of its phosphorescence spectrum in butyronitrile at 77 K, while the normalized UV absorption and fluorescence spectra made it possible to determine the approximate E_S values (350 kJ mol^{-1}). Because a singlet–singlet energy transfer from BP to *anti*-**1b** is highly endothermic (UV spectral analysis), the observed phosphorescence quenching is due to an exothermic energy transfer between triplet BP and *anti*-**1b**. The magnitude of the rate constant for a triplet–triplet energy transfer (1.3×10^7 dm^3 mol^{-1} s^{-1}) clearly shows that the triplet energy transfer takes place efficiently. It is worth noting that the energy-transfer efficiency for the present system is greater than that for the previously studied system by about an order of magnitude [16,17].

In order to estimate the extent to which the sensitized reaction proceeds *via* the triplet *syn*-isomer, the time course of this isomer concentration was followed with *anti*-**1b** (1.0×10^{-3} mol dm^{-3}) as the starting oxime derivative (Fig. 4). Inspection of changes in both the isomer concentrations confirms that the increment of *syn*-**1b** is smaller than the decrement of *anti*-**1b** by a factor of about 5 at the 5 min irradiation. In addition, the contribution of the reaction taking place through the triplet *syn*-isomer is considered to be negligible at low conversions of the latter isomer (<20%), thus allowing us to propose Scheme 2. Application of the steady-state approximation to this Scheme enabled the derivation of Eqs. (1)–(3), where Φ_{-1}, Φ_2, and $\Phi_{\text{syn-1}}$ refer to the quantum yields for disappearance of *anti*-**1** and for appearance

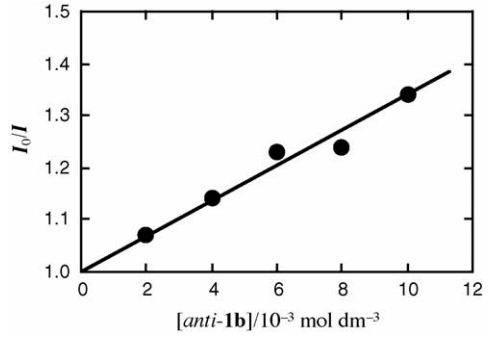

Fig. 3. Stern–Volmer plot for the phosphorescence quenching of BP (0.030 mol dm^{-3}) by *anti*-**1b** in N_2-saturated MeCN at room temperature. Excitation wavelength is 366 nm.

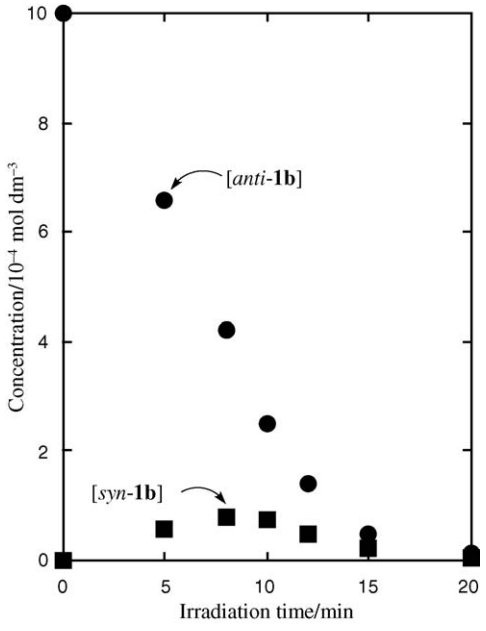

Fig. 4. Concentration of the starting *anti*-**1b** (●) and its isomer *syn*-**1b** (■) in MeCN as a function of irradiation time.

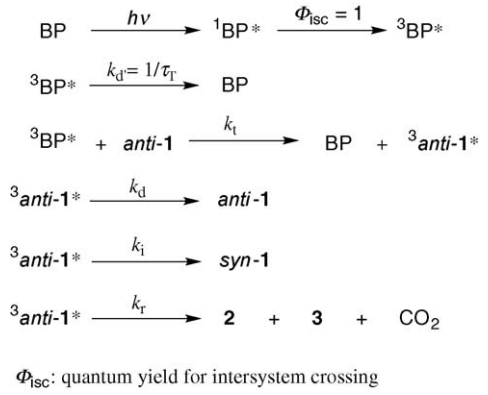

Scheme 2. Reaction scheme for the BP-sensitized photolysis of *anti*-**1**.

of **2** and *syn*-**1**, respectively:

$$\frac{1}{\Phi_{-\mathbf{1}}} = \left\{1 + \frac{k_d}{k_i + k_r}\right\}\left\{1 + \frac{1}{k_t\tau_T[anti{-}\mathbf{1}]}\right\} \quad (1)$$

$$\frac{1}{\Phi_{syn-\mathbf{1}}} = \left\{1 + \frac{k_d + k_r}{k_i}\right\}\left\{1 + \frac{1}{k_t\tau_T[anti{-}\mathbf{1}]}\right\} \quad (2)$$

$$\frac{1}{\Phi_{\mathbf{2}}} = \left\{1 + \frac{k_d + k_i}{k_r}\right\}\left\{1 + \frac{1}{k_t\tau_T[anti{-}\mathbf{1}])}\right\} \quad (3)$$

As typically shown in Fig. 5, there were good linear relationships between the reciprocals of Φ (Φ^{-1}) and concentrations of *anti*-**1** ([**1**]$^{-1}$). The same linear relationships were observed for the other derivatives and in other solvents, 1,2-dichloroethane and toluene. From the intercepts of linear plots obtained, we are able to estimate the limiting quantum yields, i.e., the quantum yields extrapolated to infinite concentrations of *anti*-**1a–e**, for disappearance of these isomers ($\Phi_{-\mathbf{1},\mathrm{lim}}$) and for formation of *syn*-**1a–e** ($\Phi_{syn\text{-}\mathbf{1},\mathrm{lim}}$) and **2** ($\Phi_{\mathbf{2},\mathrm{lim}}$). These limiting quantum yields are collected in Table 1 along with the $k_i/(k_d + k_r)$ and $k_r/(k_d + k_i)$ values that were evaluated based on the relations, $1/\Phi_{syn\text{-}\mathbf{1},\mathrm{lim}} = 1 + (k_d + k_r)/k_i$ and $1/\Phi_{\mathbf{2},\mathrm{lim}} = 1 + (k_d + k_i)/k_r$,

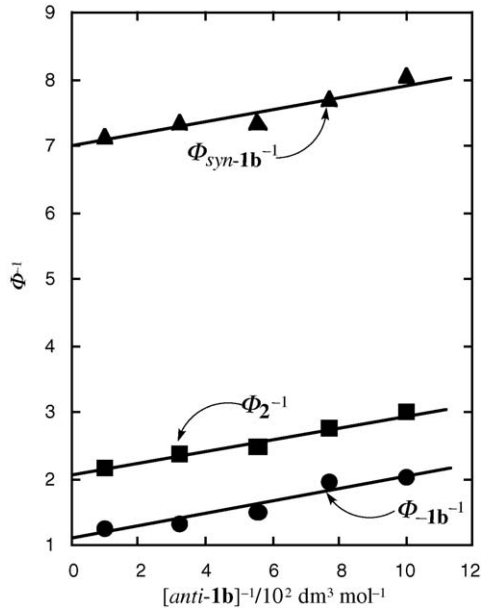

Fig. 5. Stern–Volmer plots of $\Phi_{-\mathbf{1b}}{}^{-1}$(●), $\Phi_{\mathbf{2}}{}^{-1}$(■), and $\Phi_{\text{syn-}\mathbf{1b}}{}^{-1}$(▲) vs. [*anti*-**1b**]$^{-1}$ for the BP (0.030 mol dm^{-3})-sensitized photolysis of *anti*-**1b** with 366 nm light in N_2-saturated MeCN at room temperature.

respectively. In these relations k_r is the rate constant for homolytic bond cleavage in triplet *anti*-**1**, k_d the rate constant for deactivation of the triplet *anti*-isomer, and k_i is the rate constant for isomerization of triplet *anti*-**1** into *syn*-**1**. The parameter related to $\Phi_{-\mathbf{1},\mathrm{lim}}$ was omitted for its relatively large experimental error.

2.3. Substituent and solvent effects on limiting quantum yields for the sensitized photolysis

In our previous studies [16,17], it was shown that triplet–triplet energy transfer between BP ($E_T = 290$ kJ mol^{-1}) and *N*,*N*-dibenzyl-*O*-(4-substituted benzoyl)hydroxylamines

Table 1
Substituent and solvent effects on the quantum yields and relative rates for the BP-sensitized photolysis of **1a–e** under nitrogen at room temperature

Compound	Solvent	$\Phi_{-\mathbf{1},\mathrm{lim}}$	$\Phi_{\text{syn-}\mathbf{1},\mathrm{lim}}$	$\Phi_{\mathbf{2},\mathrm{lim}}$	$\Phi_{\mathbf{3}}$[a]	$k_i/(k_d + k_r)$	$k_r/(k_d + k_i)$
1a	MeCN	0.91	0.14	0.41	0.41	0.16	0.68
1b	MeCN	0.93	0.14	0.49	0.41	0.17	0.95
1c	MeCN	0.66	0.14	0.34	–[b]	0.17	0.52
1d	MeCN	0.81	0.14	0.44	–[b]	0.16	0.80
1e	MeCN	0.83	0.14	0.46	0.35	0.17	0.84
1a	CH_2ClCH_2Cl	0.87	0.13	0.40	–[c]	0.15	0.68
1b	CH_2ClCH_2Cl	0.91	0.14	0.47	–[c]	0.16	0.90
1c	CH_2ClCH_2Cl	0.61	0.14	0.37	–[b]	0.17	0.60
1d	CH_2ClCH_2Cl	0.88	0.14	0.53	–[b]	0.16	1.11
1e	CH_2ClCH_2Cl	0.79	0.14	0.45	–[c]	0.16	0.81
1a	Toluene	0.93	0.15	0.48	–[c]	0.17	0.93
1b	Toluene	0.95	0.14	0.46	–[c]	0.16	0.85
1c	Toluene	0.58	0.13	0.31	–[b]	0.15	0.46
1d	Toluene	0.90	0.14	0.43	–[b]	0.17	0.75
1e	Toluene	0.91	0.14	0.44	–[c]	0.17	0.77

[a] Determined at [*anti*-**1**] = 1.0×10^{-2} mol dm^{-3}.
[b] Could not be determined even at [*anti*-**1**] = 1.0×10^{-2} mol dm^{-3}.
[c] Not determined.

(E_T = 280–289 kJ mol^{-1}) proceeds at the rate (k_t = 1.8–2.4 × 10^6 dm^3 mol^{-1} s^{-1}), which is much smaller than the diffusion-controlled rate (k_{DIF} = 2.9 × 10^{10} dm^3 mol^{-1} s^{-1} in MeCN at 25 °C [19]). Because both molecules have almost the same triplet energies ($\Delta E_T \approx 0$ kJ mol^{-1}), reversible energy transfer may be responsible for the slow transfer rate observed for this system. In addition, the large exothermicity for energy-transfer process between triplet BP and *N*,*N*-bis(4-substituted benzyl)-*O*-(1-naphthoyl)hydroxylamines (ΔE_T = 76–80 kJ mol^{-1}) renders this process energetically very favorable [18], and was consistent with the fact that highly exothermic triplet–triplet energy transfer proceeds at the diffusional rate and is insensitive to an electronic configurational change which occurs during this energy transfer [21]. Thus, the magnitude of ΔE_T = 21 kJ mol^{-1} for the *anti*-**1b**/BP system allows us to predict that the energy transfer takes place with a moderate efficiency. The energy-transfer rate constant of 1.3 × 10^7 dm^3 mol^{-1} s^{-1} for this system is in conformity with this prediction, indicating the triplet energy to be mainly localized in the naphthylimino moiety of **1**.

An analysis of the quantum yields for formation of **2** ($\Phi_{\mathbf{2},lim}$ = 0.34–0.49 in MeCN, see Table 1), *syn*-**1** ($\Phi_{syn\text{-}\mathbf{1},lim}$ = 0.14), and **3** ($\Phi_{\mathbf{3}}$ = 0.35–0.41) suggests that the triplet-state reactivity of *anti*-**1** is high and the triplet energy in this starting isomer is mainly utilized to cause the homolytic N–O bond cleavage and then the exclusive decarboxylation of the resulting aroyloxyl radical. In addition, any limiting quantum yields are subject to, if any, only small substituent and solvent polarity effects, being in contrast with the limiting quantum yields observed for the *N*,*N*-dibenzyl-*O*-(4-substituted benzoyl)hydroxylamine/BP system [16,17]. If we take into account the previous finding that the contribution of an ionic transition-state structure for the N–O bond cleavage in the triplet excited state is responsible for the substituent and solvent polarity dependence of these Φ_{lim} values, the above result might indicate the negligible contribution of an ionic structure to the transition state for this bond cleavage in the triplet-state *anti*-isomer.

It was previously demonstrated that the 4-toluoyloxyl radical [generated from the BP-sensitized photolysis of *N*,*N*-dibenzyl-*O*-(4-toluoyl)hydroxylamine [16,17] and *N*-(1-naphthoyl)-*N*-phenyl-*O*-(4-toluoyl)hydroxylamine [14,15]] undergoes both hydrogen abstraction and decarboxylation reactions giving 4-toluic acid and toluene in comparable quantum yields, respectively. Because these two sensitized reactions proceed through geminate radical pair intermediates, the appearance of the former product reveals that decarboxylation of the toluoyloxyl radical is not so much fast. Thus, the observation of exclusive decarboxylation of this radical in the *anti*-**1b**/BP system allows us to propose that toluene is formed via hydrogen abstraction of the tolyl radical (which is obtained by the simultaneous N–O and C(=O)–Ar bond cleavages in the triplet-state *anti*-**1b**) but not via decarboxylation of the toluoyloxyl radical. The precedent of such a two bond cleavage mode is found in the photodecomposition of aroyl peroxide where the O–O and C(=O)–Ar bond fissions take place simultaneously in the excited state to afford carbon dioxide, aroyloxyl and aryl radicals [22–24]. It is very likely that triplet excitation energy localized in the naphthylimino moiety is efficiently converted into the vibrational energy of the N–O–C(=O)–Ar bond in the triplet excited-state **1**.

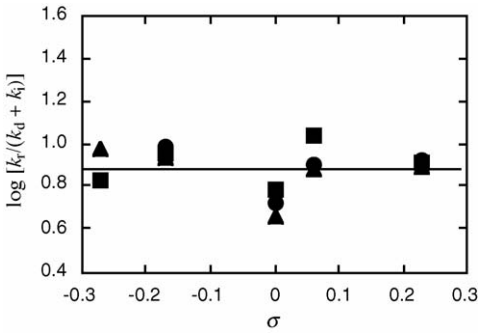

Fig. 6. Correlation of log [k_r/(k_d + k_i)] with σ values for the BP-sensitized photolysis of *anti*-**1** with 366 nm light in MeCN (●), CH_2ClCH_2Cl (■), and toluene (▲).

A Hammett analysis of the correlation of rates with substituent constants provides significant information about the transition-state structure for both heterolytic and homolytic cleavages of a specific bond [25]. It was previously found that the triplet-state deactivation (k_d) of a given model hydroxylamine should undergo a much less sensitive electronic effect of the substituent than the N–O bond cleavage process (k_r) does, thus allowing us to use the k_r/k_d value for the Hammett analysis [16–18]. The finding that the relative rates $k_i/(k_d + k_r)$ and $k_r/(k_d + k_i)$ are influenced by the electronic property of a given substituent and the polarity of a given solvent to, if any, only a small extent (Table 1) strongly suggests that the substituent exerts a negligible effect not only on the rate constant k_d but also on the k_i. Based on this finding we were led to conclude that the $k_r/(k_d + k_i)$ value may be used for making the Hammett plot. An analysis of the plots given in Fig. 6 confirmed that the magnitude of log [k_r/(k_d + k_i)] shows a negligible dependence on the substituent constant σ in any solvents. Thus, taking into consideration the simultaneous two bond cleavages, we are able to propose the transition-state structure **I** (Chart 2) to which an ionic structure contributes to a negligible extent, as already suggested. If we accept this transition-state structure for the N–O bond cleavage process in the triplet excited state, the initially formed triplet radical pair **II** is very likely to undergo efficient intersystem crossing to the corresponding singlet radical pair

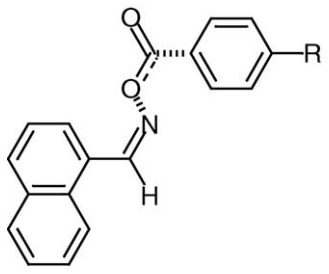

I

Chart 2.

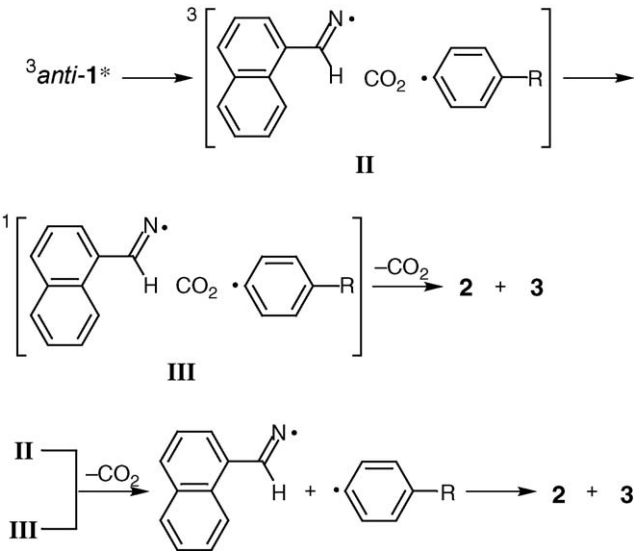

Scheme 3. Reaction mechanism proposed for the nitrile-forming radical elimination of *anti*-**1** activated by triplet BP.

III. As judged from the previously obtained mechanistic information, the elimination product **2** are considered to be mostly derived from hydrogen abstraction of the aryl radical from the naphthylmethyleneimino radical in the latter caged radical pair intermediate **III**. In addition to the intersystem crossing from **II** to **III**, this hydrogen abstraction takes place, of course, in competition with the diffusive separation of the caged radicals, as shown in Scheme 3.

3. Experimental

3.1. Measurements

High-performance liquid chromatography (HPLC) analysis of the photoproducts was performed on a Shimadzu Model LC-10AT$_{VP}$ high-performance liquid chromatograph equipped with a 4.6 mm × 250 mm ODS (Zorbax) column and a Shimadzu Model SPD-10A$_{VP}$/10AV$_{VP}$ UV detector (detection wavelength, 240 nm; mobile phase, MeCN:H_2O = 60:40 v/v). Infrared (IR) spectra were taken with a Shimadzu Model IRPrestige-21 infrared spectrophotometer. Nuclear magnetic resonance (NMR) spectra were recorded on a JEOL Model JNM-A500 spectrometer. Chemical shifts (in ppm) were determined using tetramethylsilane as an internal standard. In addition to the fluorescence of the starting *O*-acyloxime derivative, the room-temperature phosphorescence of benzophenone with and without this oxime derivative was measured under nitrogen with a Hitachi Model F-4500 spectrofluorimeter. Gas liquid chromatography (GLC) analysis of the photoproducts was carried out on a Shimadzu Model CR-6A gas chromatograph equipped with a 3 mm × 3000 mm glass column (10% silicon SE30 on 60–80 mesh Uniport B) and a FID. Ultraviolet (UV) spectra were taken on a Hitachi Model U-3300 spectrophotometer. MM2 and PM5 calculations were accomplished by using CAChe 5.0 for Windows available from Fujitsu Ltd., 2002.

3.2. Materials and solvents

1-Naphthaldehyde oxime was prepared from the condensation reaction of 1-naphthaldehyde with hydroxylamine in refluxing ethanol. *O*-acylation of this oxime with 4-substituted benzoyl chlorides in dichloromethane containing equimolecular amounts of triethylamine gave 1-naphthaldehyde *O*-(4-substituted benzoyl)oximes in greater than 82% yields. The crude products were purified by column chromatography over silica gel (70–230 mesh, Merck) using chloroform as an eluent, followed by recrystallization from ethyl acetate–hexane to afford colorless crystals with the following physical and spectroscopic properties.

3.2.1. 1-Naphthaldehyde O-(4-anisoyl)oxime (*1a*)

The m.p. 88.0–89.0 °C; IR (KBr) ν: 1731, 1608 cm^{-1}; ^{1}H NMR (500 MHz, $CDCl_3$) δ: 3.89 (3H, s), 6.99 (2H, d, J = 6.7 Hz), 7.54 (1H, dd, J = 6.1, 6.1 Hz), 7.57 (1H, dd, J = 7.9, 8.5 Hz), 7.66 (1H, dd, J = 7.9, 8.5 Hz), 7.92 (1H, d, J = 8.5 Hz), 7.98 (1H, d, J = 6.1 Hz), 7.99 (1H, d, J = 6.1 Hz), 8.14 (2H, d, J = 6.7 Hz), 8.71 (1H, d, J = 8.5 Hz), 9.15 (1H, s); ^{13}C NMR (125 MHz, CDCl3) δ: 55.52, 113.93 (2C), 120.96, 124.76, 125.21, 126.38, 126.53, 127.90, 128.88, 129.72 (2C), 130.92, 131.89 (2C), 132.86, 133.84, 156.32, 163.80. Analysis: calculated for $C_{19}H_{15}NO_3$: C, 74.74%; H, 4.95%; N, 4.59%; found: C, 74.73%; H, 4.86%; N, 4.59%.

3.2.2. 1-Naphthaldehyde O-(4-toluoyl)oxime (*1b*)

The m.p. 117.0–118.0 °C; IR (KBr) ν: 1740, 1608 cm^{-1}; ^{1}H NMR (500 MHz, $CDCl_3$) δ:2.45 (3H, s), 7.31 (2H, d, J = 8.2 Hz), 7.53 (1H, dd,J = 6.1, 7.6 Hz), 7.55 (1H, dd, J = 7.0, 7.6 Hz), 7.66 (1H, dd, J = 7.0, 8.5 Hz), 7.91 (1H, d, J = 7.6 Hz), 7.97 (1H, d, J = 6.1 Hz), 7.99 (1H, d, J = 7.6 Hz), 8.08 (2H, d, J = 8.2 Hz), 8.71 (1H, d, J = 8.5 Hz), 9.16 (1H, s); ^{13}C NMR (125 MHz, $CDCl_3$) δ: 21.75, 124.77, 125.21, 125.97, 126.33, 126.53, 127.92, 128.88, 129.34 (2C), 129.77, 129.83 (2C), 130.93, 132.41, 133.85, 144.24, 156.52, 164.12. Analysis: calculated for $C_{19}H_{15}NO_2$: C, 78.87%; H, 5.23%; N, 4.84%; found: C, 78.58%; H, 5.32%; N, 4.85%.

3.2.3. 1-Naphthaldehyde O-benzoyloxime (*1c*)

The m.p. 127.0–127.5 °C; IR (KBr) ν: 1746, 1584 cm^{-1}; ^{1}H NMR (500 MHz, $CDCl_3$) δ: 7.52 (2H, dd, J = 7.3, 7.9 Hz), 7.55 (1H, dd, J = 7.3, 7.9 Hz), 7.58 (1H, dd, J = 7.9, 8.5 Hz), 7.63 (1H, dd, J = 7.3, 7.3 Hz), 7.67 (1H, dd, J = 7.9, 8.5 Hz), 7.92 (1H, d, J = 8.5 Hz), 7.98 (1H, d, J = 7.3 Hz), 8.00 (1H, d, J = 7.9 Hz), 8.19 (2H, d, J = 7.9 Hz), 8.72 (1H, d, J = 8.5 Hz), 9.17 (1H, s); ^{13}C NMR (125 MHz, $CDCl_3$) δ: 124.76, 125.20, 126.22, 126.56, 127.96, 128.62, 128.78 (2C), 128.90, 129.79 (2C), 129.87, 130.91, 132.50, 133.44, 133.84, 156.75, 164.04. Analysis: calculated for $C_{18}H_{13}NO_2$: C, 78.53%; H, 4.76%; N, 5.09%; found: C, 78.65%; H, 4.74%; N, 4.97%.

3.2.4. 1-Naphthaldehyde O-(4-fluorobenzoyl)oxime (*1d*)

The m.p. 135.5–136.0 °C; IR (KBr) ν: 1743, 1602 cm^{-1}; ^{1}H NMR (500 MHz, $CDCl_3$) δ: 7.19 (2H, dd, J = 9.2, 9.2 Hz), 7.54 (1H, dd, J = 7.3, 7.9 Hz), 7.58 (1H, dd, J = 7.3, 7.9 Hz),

7.67 (1H, dd, J = 7.9, 8.5 Hz), 7.92 (1H, d, J = 7.3 Hz), 7.97 (1H, d, J = 7.3 Hz), 8.00 (1H, d, J = 7.9 Hz), 8.21 (2H, dd, J = 5.5, 9.2 Hz), 8.71 (1H, d, J = 8.5 Hz), 9.15 (1H, s); ^{13}C NMR (125 MHz, $CDCl_3$) δ: 115.87 (2C, d, J = 23 Hz), 124.73, 125.01, 125.21, 126.61, 128.01, 128.93, 129.93, 129.95, 130.90, 132.35, 132.39 (2C, d, J = 10 Hz), 133.86, 156.88, 164.08 (1C, d, J = 246 Hz), 165.06. Analysis: calculated for $C_{18}H_{12}FNO_2$: C, 73.71%; H, 4.12%; N, 4.78%; found: C, 73.55%; H, 3.90%; N, 4.51%.

*3.2.5. 1-Naphthaldehyde O-(4-chlorobenzoyl)oxime (**1e**)*

The m.p. 127.0–128.0 °C; IR (KBr) ν: 1746, 1587 cm^{-1}; ^{1}H NMR (500 MHz, $CDCl_3$) δ: 7.49 (2H, d, J = 8.5 Hz), 7.55 (1H, dd, J = 7.3, 7.9 Hz), 7.58 (1H, dd, J = 7.9, 8.5 Hz), 7.67 (1H, dd, J = 7.9, 8.5 Hz), 7.92 (1H, d, J = 8.5 Hz), 7.97 (1H, d, J = 7.3 Hz), 8.00 (1H, d, J = 7.9 Hz), 8.12 (2H, d, J = 8.5, Hz), 8.70 (1H, d, J = 8.5 Hz), 9.16 (1H, s); ^{13}C NMR (125 MHz, $CDCl_3$) δ: 124.72, 125.21, 126.05, 126.61, 127.20, 128.01, 128.93, 129.01 (2C), 129.96, 130.89, 131.15 (2C), 132.63, 133.85, 139.98, 156.32, 163.80. Analysis: calculated for $C_{18}H_{12}ClNO_2$: C, 69.80%; H, 3.90%; N, 4.52%; found: C, 69.62%; H, 3.73%; N, 4.43%.

In order to isolate and characterize the *syn*-isomer, an acetonitrile solution of *anti*-**1b** (100 mL, 1.0×10^{-3} mol dm^{-3}) placed in a Pyrex vessel was irradiated for 60 min under nitrogen at room temperature with Pyrex-filtered light from a 450 W high-pressure Hg lamp (external irradiation). The irradiated solution was concentrated to dryness in vacuo and the resulting residue was dissolved in chloroform-*d* to measure ^{1}H and ^{13}C NMR spectra. A comparison of the NMR spectra of *anti*-**1b** with those of this residue enabled the assignment of NMR signals for *syn*-**1b**.

*3.2.6. Syn-**1b***

^{1}H NMR (500 MHz, $CDCl_3$) δ: 2.35 (3H, s), 7.14 (2H, d, J = 8.2 Hz), 7.52–7.57 (2H, m), 7.65–7.68 (1H, m), 7.87 (1H, d, J = 7.6 Hz), 7.92–7.95 (2H, m), 8.00 (2H, d, J = 8.2 Hz), 8.25 (1H, d, J = 8.5 Hz), 8.62 (1H, s); ^{13}C NMR (125 MHz, $CDCl_3$) δ: 21.67, 124.18, 124.95, 125.62, 127.39, 127.58, 127.74, 128.63, 128.67 (2C), 128.80, 129.22 (2C), 129.82, 130.25, 132.66, 133.30, 144.53, 153.03, 163.88.

Benzophenone and 4-substituted benzoic acids were purified by recrystallization from ethanol and aqueous ethanol, respectively. 1-Cyanonaphthalene, anisole, and chlorobenzene were of the highest grade available and used without further purification. 1,2-Dichloroethane and toluene were of spectroscopic grade and used as received. Purification of acetonitrile was accomplished by the standard method [26].

3.3. Quantum yields

A potassium tris(oxalato)ferrate(III) actinometer was employed to determine the quantum yields for the benzophenone-sensitized nitrile-forming radical elimination at low conversions (<20%) of the starting 1-naphthaldehyde *O*-aroyloximes **1a**–**e** [27]. A 450 W high-pressure Hg lamp was used as the light source from which 366 nm light for the photolysis was selected with Corning 0-52, Corning 7-60, and Toshiba IRA-25S glass filters. Linear calibration curve for each compound, made under the same analytical conditions, was utilized to quantify the disappearance of *anti*-**1** and appearance of *syn*-**1**, **2**, and **3**. All of the quantum yields are an average of more than five determinations.

Acknowledgement

This research was partially supported by a "High-Tech Research Center Project" from the Ministry of Education, Culture, Sports, Science and Technology, Japan.

References

[1] S. Oae, T. Sakurai, Bull. Chem. Soc. Jpn. 49 (1976) 730.
[2] R.V. Hoffman, R.A. Bartsch, B.R. Cho, Acc. Chem. Res. 22 (1989) 211, and references cited therein.
[3] B.R. Cho, S.Y. Pyun, J. Am. Chem. Soc. 113 (1991) 3920.
[4] F.M. Bickelhaupt, L.J. de Koning, N.M.M. Nibbering, J. Org. Chem. 58 (1993) 2436.
[5] Q. Meng, A. Thibblin, J. Am. Chem. Soc. 119 (1997) 1224.
[6] S.Y. Pyun, D.C. Lee, Y.J. Seung, B.R. Cho, J. Org. Chem. 70 (2005) 5327.
[7] B.R. Cho, N.S. Cho, S.K. Lee, J. Org. Chem. 62 (1997) 2230, and references cited therein.
[8] B.R. Cho, N.S. Cho, K.S. Song, K.N. Son, Y.K. Kim, J. Org. Chem. 63 (1998) 3006.
[9] B.R. Cho, H.S. Chung, N.S. Cho, J. Org. Chem. 63 (1998) 4685.
[10] B.R. Cho, N.S. Cho, S.H. Song, S.K. Lee, J. Org. Chem. 63 (1998) 8304.
[11] F.G. Bordwell, Acc. Chem. Res. 5 (1972) 374.
[12] W.H. Saunders Jr., Acc. Chem. Res. 9 (1976) 19.
[13] R.A. Bartsch, J. Závada, Chem. Rev. 80 (1980) 453.
[14] T. Sakurai, H. Yamamoto, S. Yamada, H. Inoue, Bull. Chem. Soc. Jpn. 58 (1985) 1174.
[15] T. Sakurai, H. Sukegawa, H. Inoue, Bull. Chem. Soc. Jpn. 58 (1985) 2875.
[16] T. Sakurai, H. Mizuno, T. Kubota, H. Inoue, Bull. Chem. Soc. Jpn. 64 (1991) 2140.
[17] T. Nishijima, T. Ohishi, K. Kubo, T. Sakurai, H. Inoue, Nippon Kagaku Kaishi (1996) 882.
[18] F. Andoh, K. Kubo, T. Sakurai, Bull. Chem. Soc. Jpn. 72 (1999) 2537.
[19] S.L. Murov, I. Carmichael, G.L. Hug, Handbook of Photochemistry, 2nd ed., Marcel Dekker, New York, 1993.
[20] T. Arai, T. Wakabayashi, H. Sakuragi, K. Tokumaru, Chem. Lett. (1985) 279.
[21] N.J. Turro, Modern Molecular Photochemistry, Benjamin/Cummings, Menlo Park, California, 1978, pp. 296–361.
[22] A. Kitamura, H. Sakuragi, M. Yoshida, K. Tokumaru, Bull. Chem. Soc. Jpn. 53 (1980) 1393.
[23] T. Najiwara, J. Hashimoto, K. Segawa, H. Sakuragi, Bull. Chem. Soc. Jpn. 76 (2003) 575.
[24] B. Abel, J. Aβmann, M. Buback, M. Kling, S. Schmatz, J. Schroeder, Angew. Chem. Int. Ed. 42 (2003) 300.
[25] N.S. Isaacs, Physical Organic Chemistry, Longman Scientific & Technical, Essex, 1987.
[26] J.A. Riddick, W.B. Bunger, T.K. Sakano, Organic Solvents, 4th ed., Wiley, Chichester, 1986.
[27] C.G. Hatchard, C.A. Parker, Proc. Roy. Soc. London Ser. A 235 (1956) 518.